

# DFT+ $U$ search for the energy minimum among eight collinear and noncollinear magnetic structures of $\text{GdB}_4$

Muhammad N. Huda\* and Leonard Kleinman

*Department of Physics, University of Texas at Austin, Austin, Texas 78712, USA*

(Received 7 December 2007; revised manuscript received 20 August 2008; published 30 September 2008)

We have studied eight collinear and noncollinear magnetic orientations of  $\text{GdB}_4$  using the GGA+ $U$  method, without and with spin-orbit coupling, for values of  $U-J$  between 0 and 6. For  $U-J=6$ , the value which had been found to yield the correct Gd lattice constants, we obtain  $\text{GdB}_4$  lattice constants within 0.26% of experiment. We find that the magnetization lies in plane but is collinear, in disagreement with the most recent experimental determination.

DOI: [10.1103/PhysRevB.78.094424](https://doi.org/10.1103/PhysRevB.78.094424)

PACS number(s): 75.25.+z, 75.50.Ee, 71.20.Eh

## I. INTRODUCTION

Elements and compounds of the lanthanide series in the Periodic Table are characterized by the presence of localized  $4f$  electrons. The magnetic properties of these materials and their compounds primarily depend on these  $f$  electrons and their coupling to each other through indirect exchange mechanisms.<sup>1</sup> Due to their narrow  $4f$  bands, these electrons are strongly correlated and can show heavy fermion behavior. Various magnetic phases<sup>2</sup> and superconductivity are also found in these systems due to the complex behavior of those electrons. Gadolinium (Gd) sits in the middle of the lanthanide series and has a half-filled  $4f$  electron shell. Metallic Gd is a ferromagnet with a magnetic moment of  $7.63 \pm 0.01 \mu_B$ /atom and the compounds of Gd have shown very interesting magnetic behavior. For example, Gd mononitrides are in general antiferromagnetic but show high sensitivity to stoichiometry and external magnetic field.<sup>3</sup>

All rare-earth elements,  $\text{NdB}_4$  through  $\text{TmB}_4$ , except Eu form isostructural antiferromagnetic metallic tetraborides crystallizing at room temperature in the space group  $P4/mbm$ .<sup>4,5</sup> Susceptibility measurements<sup>4</sup> indicate that all except  $\text{TmB}_4$  and  $\text{GdB}_4$  polarize along the fourfold axis, while the Tm and Gd magnetic vectors lie in the perpendicular plane.  $\text{CeB}_4$  and  $\text{YbB}_4$  do not order magnetically and  $\text{PrB}_4$  is a ferromagnet. Using spherical neutron polarimetry, Blanco *et al.*<sup>6</sup> determined a particular orientation for the Gd magnetization vectors in the 4 f.u. unit cell. We cannot judge the accuracy of their determination but we observed that Blanco *et al.*<sup>6</sup> reported only ambient temperature lattice constants and atomic positions within the unit cell obtained by Garland *et al.*<sup>7</sup> and none at 2.2 K. Blanco *et al.*<sup>6</sup> also stated that its space group is  $P4/mbm$  at room temperature, leading us to wonder whether they accurately determined the crystal structure at 2.2 K where their measurements were made. A small distortion of the lattice away from fourfold symmetry would eliminate the possibility of the noncollinear magnetic structures they consider. We also note that, based on x-ray data,<sup>8</sup> two of the authors<sup>5</sup> concluded that a structural phase transition occurred at a temperature above the magnetic transition; from the tetragonal  $P4/mbm$  structure to the orthorhombic  $P2_12_12$ , although later,<sup>9</sup> using the same data, they concluded that there was no phase transition. In an attempt to verify the ground-state structure in Ref. 6 we have calculated

the total energy of four collinear and four noncollinear possible magnetic structures of  $\text{GdB}_4$ . In Sec. II we discuss the failure of ordinary density-functional theory (DFT) to reproduce the correct electronic structure of Gd and the computational method used here. In Sec. III our results and conclusions are presented and in the Appendix we describe the five possible color (i.e., magnetic) groups according to which  $\text{GdB}_4$  could transform if it maintains its  $P4/mbm$  structure below  $T_N$ .

## II. COMPUTATIONAL METHOD

It is well known that the local spin-density approximation (LSDA) and generalized gradient approximation (GGA) of DFT do not reproduce the correct band structure for Gd. This manifests itself in majority-spin  $4f$  bands too high in the valence bands and minority-spin  $4f$  bands just above the Fermi surface, so that their hybridization therein results in much too large a Fermi-surface density of states (DOS). Some time ago Bylander and Kleinman<sup>10</sup> determined that an atomic Hartree-Fock (HF) calculation resulted in vastly lower energy occupied  $4f$  states and higher lying unoccupied  $4f$  states than a DFT calculation did. Treating the majority spin  $4f$ 's as core states, they constructed an HF core/LSDA valence electron pseudopotential, which resulted in Gd lattice constants in near perfect agreement with experiment and a DOS at the Fermi energy that was actually somewhat less than the experimental value.<sup>11</sup> There were two shortcomings to this calculation, which in hindsight could have been avoided. First, in order to obtain the experimental magnetization, a parameter screening the *difference* between majority and minority-spin exchange-correlation potentials had to be introduced. When the value of the parameter determined in the bulk calculation was used in a thin-film calculation,<sup>12</sup> excellent agreement with experiment was obtained for the surface plane relaxation. The use of a screening parameter could have been avoided if instead of taking  $V_{xc}(\text{val}) = V_{xc}(\rho_{\text{val}})$ , they had taken  $V_{xc}(\text{val}) = V_{xc}(\rho_{\text{tot}}) - V_{xc}(\rho_{\text{core}})$ . Second, the minority-spin  $4f$  bands were free-electron-like rather than sharp resonances. This was a consequence of using a pseudopotential whose range was not short enough to induce a resonance and could be overcome at the expense of extremely poor convergence, with a short-range pseudopo-

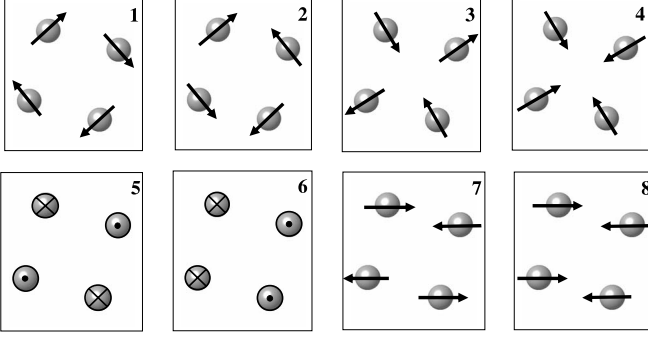


FIG. 1. Eight possible Gd spin arrangements for  $\text{GdB}_4$ . The first five transform according to magnetic groups of the  $P4/mbm$  space group.

tential. It could also be avoided by using the Vanderbilt<sup>13</sup> ultrasoft pseudopotential or any all-electron method which had been modified so that the core-core and core-valence exchange interactions were HF and the valence-valence were LSDA.

Petersen, Hafner, and Marsman<sup>14</sup> (PHM) recently made an extensive study of bulk Gd and its surface using the Vienna *ab initio* simulation package, VASP(4.6.21),<sup>15–18</sup> with the DFT+ $U$  method and the projected augmented wave (PAW) expansion<sup>19</sup> in agreement with experiment for the  $4f$  spin splitting with  $U-J=7$  eV and for the magnetization and unit-cell volume with  $U-J\approx 5.7$  eV. Both the DFT+ $U$  and HF methods increase the DFT lattice constants, lower the majority-spin  $4f$  eigenvalues, and raise the minority-spin  $4f$  eigenvalues; but, paradoxically, DFT+ $U$  does this by *adding* a repulsive correlation term to the DFT energy functional, while HF does it by *eliminating* the repulsive DFT self-energy. Thus, both work but for entirely different physical reasons. The VASP PAW DFT+ $U$  method has the advantage over our previous method that it treats the majority-spin  $4f$  electrons as crystal valence electrons rather than atomic core electrons and is the method we will use for  $\text{GdB}_4$ . The DFT+ $U$  functional is<sup>20</sup>

$$E_{\text{DFT}+U} = E_{\text{DFT}} + \frac{1}{2}(U-J) \sum_{\sigma} \text{Tr}(\rho^{\sigma} - \rho^{\sigma} \rho^{\sigma}). \quad (1)$$

Here  $U$  and  $J$  are screened exchange and Coulomb integrals and  $\rho^{\sigma}$  is the density matrix of the  $4f$  electrons with spin  $\sigma$ . Attempts to calculate  $U$  and  $J$  from first principles have proved unfruitful<sup>21</sup> and they are almost always treated as a single empirical parameter. Upon taking the functional derivative, the potential,

TABLE I. Lattice constants of noncollinear  $\text{GdB}_4$   $P4/mbm$  unit cells for different values of  $U-J$  (in eV) and the average of the magnetization projected on the four Gd atoms, without and with (spin orbit), compared with the experimental values.

$U-J$	$a$ (Å)	$c$ (Å)	$M$ ( $\mu_B$ )
0	7.115	4.034	6.939 (6.888)
2	7.118	4.036	7.016 (7.000)
3	7.120	4.038	7.041 (7.030)
4	7.122	4.039	7.060 (7.053)
5	7.123	4.040	7.074 (7.069)
6	7.123	4.041	7.083 (7.079)
Expt.	7.132 <sup>a</sup>	4.051 <sup>a</sup>	7.14 $\pm$ 0.17 <sup>b</sup>

<sup>a</sup>Reference 6.

<sup>b</sup>Reference 5.

$$V_{\sigma ij} = V_{\text{DFT}} + (U-J) \left( \frac{1}{2} \delta_{ij} - \rho_{ij} \right), \quad (2)$$

is obtained; because no element of the diagonalized density matrix exceeds unity, the second term in the energy functional is repulsive and the second term in the potential is attractive (repulsive) for spin states more (less) than half full.

The fully unconstrained approach to noncollinear magnetism was used, where the magnetization density is calculated as a continuous vector variable of position.<sup>22</sup> This is in contrast to the atomic moment approximation where a fixed quantization direction is assumed for each atomic site. The calculations were started with the Gd spins oriented in eight different ways and fell into the local energy minimum configurations displayed in Fig. 1. The PW91 GGA density functional<sup>23</sup> was used. All plane waves up to 300 eV were included in the PAW expansion, a  $7 \times 7 \times 12$   $\mathbf{k}$ -point sampling of the Brillouin zone (BZ) was used, and the atomic positions were relaxed until all forces were less than 0.01 eV/Å. Further relaxation did not affect the total energy to the  $\mu\text{eV}$  accuracy of Table II. BZ integrations were performed using the second-order Methfessel-Paxton method.<sup>24</sup> We performed all our calculations both fully relativistically and semirelativistically, i.e., with and without spin-orbit coupling, and the spin-orbit coupling was treated self-consistently. The outer core  $5s$  and  $5p$  electrons were treated as valence electrons.

### III. RESULTS AND DISCUSSION

The first four configurations of the Gd spins in Fig. 1 are those considered in Ref. 6. Although it is oriented out of

TABLE II. Energies (in eV/unit cell) of the Gd magnetic configurations displayed in Fig. 1, relative to the experimentally determined ground state, configuration 1, for values of  $U-J$  (in eV) with spin orbit.

$U-J$	1	2	3	4	5	6	7	8
0	0	0.002108	-0.110 747	-0.227685	0.047713	0.019318	0.038402	-0.002 189
2	0	-0.016667	-0.122 314	-0.015310	0.026447	-0.001590	0.017338	-0.020 774
3	0	0.000670	0.000 882	0.001527	0.041067	0.014284	0.031948	-0.004 092
4	0	0.000567	0.000 534	0.001094	0.038919	0.013595	0.029800	-0.004 068
5	0	0.000474	0.000 335	0.000827	0.036901	0.013084	0.027773	-0.004 027
6	0	0.000054	0.000 222	0.000281	0.023095	0.000126	0.018794	-0.003 467

TABLE III. Three nearest-neighbor Gd-Gd distances are listed for  $U-J=6$  eV with spin-orbit coupling.

	1 (Å)	2 (Å)	3 (Å)
Experiment <sup>a</sup>	3.682	3.693	4.051
Configuration 1	3.692	3.686	4.041
Configuration 6	3.394	3.686	4.041
Configuration 8	3.692	3.685, 3.686	4.041

<sup>a</sup>Reference 6.

plane, we considered the fifth configuration because it is in the  $P4/mbm$  space group and the sixth because it is (according to Ref. 4) the configuration of all the tetraborides except Gd and Dy. The last two in-plane configurations were considered because we suspected one of them might be the ground-state configuration.

The lattice constants, which are independent of whether or not the spin-orbit interaction is included and which (for the four configurations considered in Ref. 6) are also configuration independent, are listed in Table I, along with the average (over configurations) of the magnitudes of the Gd projected magnetizations.  $B$  projections do not produce magnetic moments. For  $U-J=6$  eV the magnetizations are independent of configuration and spin-orbit effects are noticeable only in the third decimal place. The  $U-J=6$  eV with spin-orbit results are in superb agreement with experiment. The spin-orbit magnetizations are slightly smaller than those without spin orbit for all values of  $U-J$  because the spin-orbit interaction mixes some minority spin into the majority-spin  $f$  states. The calculated lattice constants may actually be slightly too large when one takes into account that the measured results were obtained at ambient temperature. The lattice constants of the three configurations, which do not have fourfold rotation symmetry, differ only slightly. Configurations 6 and 8, for example, have  $a=7.124$  and  $7.123$  Å, respectively,  $b=7.122$  Å, and  $c=4.041$  Å, where  $a(b)$  lies along the  $x(y)$  axis in Fig. 1.

Table II lists the energy (including spin orbit) of each configuration relative to that of configuration 1, the experimental ground state, for several values of  $U-J$ . Identical conclusions are to be drawn for any  $U-J \geq 3$  eV (and for  $U-J=6$  eV without spin orbit). The first thing to be noted is that the experimental ground state is the calculated ground state among the four noncollinear states that were considered in Ref. 6 but that the energy differences are sufficiently small that their significance could be questioned. As noted in Ref. 6, if the magnetic coupling could be described by isotropic exchange interactions between three nearest Gd neighbors, the four configurations would be exactly degenerate and the requirement for antiferromagnetism<sup>25</sup> would be  $2J_3 - J_1 > 0$ . The requirement for configurations 5 and 7 to be antiferromagnetic would be  $2J_3 - 4J_2 + J_1 > 0$  so it is not surprising that these are significantly higher in energy than the noncollinear configurations. On the other hand, configurations 6 and 8 have a requirement,  $2J_3 - J_1 + J_{2a} - J_{2b} > 0$  which is essentially equivalent to that of the noncollinear configurations, because  $J_{2a} - J_{2b}$  is vanishingly small. This follows from the negligible difference in the two neighbor (No. 2) distances listed in Table III. Thus it is not surprising that

TABLE IV. Convergence of cohesive energies of configurations 8 and 1 (for  $U-J=6$  with SO) as a function of the size of the  $k$ -point mesh used in the BZ integration.

	$k$ points	$E_8$ (eV)	$E_1$ (eV)	$(E_8 - E_1)$
$4 \times 4 \times 7$	112	-176.005 630	-176.002 931	-0.002 699
$5 \times 5 \times 9$	225	-176.024 003	-176.020 397	-0.003 606
$6 \times 6 \times 11$	396	-176.007 325	-176.004 617	-0.002 708
$7 \times 7 \times 12$	588	-176.013 699	-176.010 232	-0.003 467
$8 \times 8 \times 14$	896	-176.011 921	-176.008 959	-0.002 962
$9 \times 9 \times 16$	1296	-176.010 276	-176.007 755	-0.002 521
$11 \times 11 \times 19$	2299	-176.009 584	-176.007 146	-0.002 438

their energies are closer to those of the first four configurations than to those of configurations 5 and 7. Configuration 8 is the calculated ground state, 3.5 meV below the experimental ground state, which is calculated to be the lowest energy metastable state.

In Tables IV and V we compare the convergence of the cohesive energies<sup>26</sup> of configurations 8 ( $E_8$ ) and 1 ( $E_1$ ) as a function of the plane-wave integration mesh size and with respect to the size of the plane-wave expansion. On going from the  $7 \times 7 \times 12$  mesh to the  $11 \times 11 \times 19$  the energy difference is reduced by 1 meV, but on going from the  $9 \times 9 \times 16$  the reduction is only 0.1 meV so it is likely that the  $11 \times 11 \times 19$  mesh result is very nearly converged. The plane-wave expansion was tested with the  $9 \times 9 \times 16$  mesh. The cohesive energies dropped by 0.22 eV between the plane waves of 300 and 500 eV cutoff energies, but  $(E_8 - E_1)$  was essentially converged with 350 eV plane waves and the total change in  $(E_8 - E_1)$  is an increase of only 0.35 meV. If we add this to the  $11 \times 11 \times 19$  mesh, 300 plane-wave value of  $(E_8 - E_1)$ , we obtain  $(E_8 - E_1) = 2.8$  meV/unit cell.

We note an apparent peculiarity in Table II. Configuration 4 lies 228 meV below configuration 1 when  $U-J=0$  but lies slightly above it when  $U-J=6$  eV. This is a consequence of the spin-orbit interaction. The spin-orbit energy (the difference between the total energies without and with spin orbit) for  $U-J=6$  eV is essentially identical for configurations 4 and 1 (3.1382 and 3.1384 eV, respectively), but for  $U-J=0$ , the spin-orbit energy of configuration 4 is 230 meV larger than that of configuration 1 (2.8266 eV vs 2.5967 eV). The Hubbard  $U$  has several effects. It raises the total energy because it adds a repulsion between electrons on the same site, but this effect is reduced because, while raising the unoccupied minority-spin  $4f$  eigenvalues, it lowers the occupied majority-spin  $4f$  eigenvalues. This slightly increases the magnetization by shifting the occupied and unoccupied  $f$

TABLE V. Convergence of cohesive energies of configurations 8 and 1 (for  $U-J=6$ , with SO) as a function of plane-wave expansion cutoff energy in eV.

$E$ cut	$E_8$ (eV)	$E_1$ (eV)	$(E_8 - E_1)$ (eV)
300	-176.010 276	-176.007 755	-0.002 521
350	-176.189 340	-176.186 512	-0.002 828
400	-176.222 997	-176.220 153	-0.002 844
450	-176.226 827	-176.223 967	-0.002 860
500	-176.236 660	-176.233 790	-0.002 870

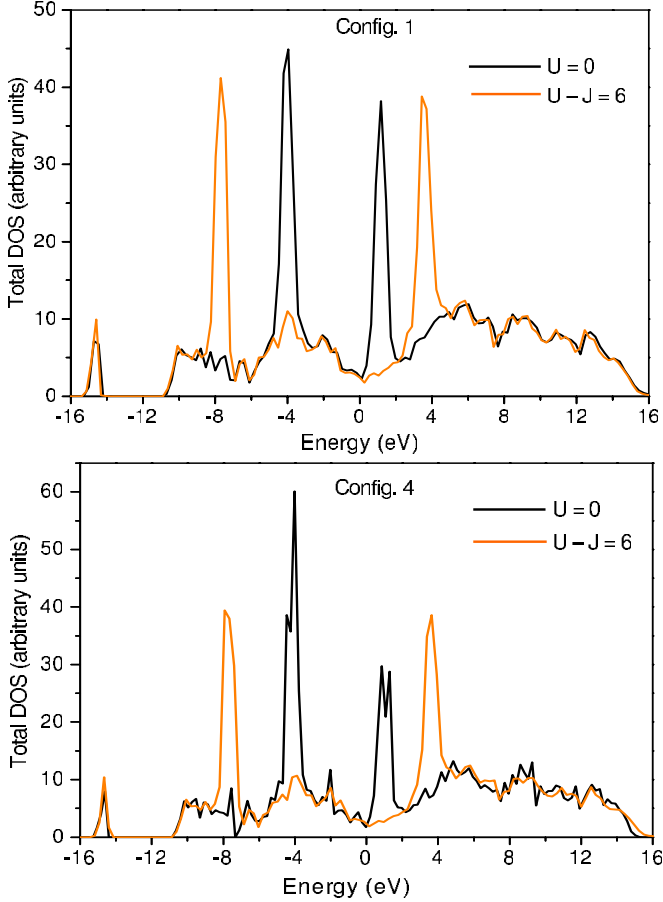


FIG. 2. (Color online) Total densities of states for configurations 1 and 4 of Fig. 1 for  $U-J=0$  and 6 with spin-orbit included. The Fermi energy is at  $E=0$ .

bands away from the Fermi energy and thus reducing the hybridization of the majority spin  $4f$ 's out of and the minority spin  $4f$ 's into the occupied bands. The splitting of the majority and minority  $4f$  eigenvalues significantly reduces their contribution to the spin-orbit energy. This is demonstrated in Fig. 2 where the  $U-J=0$  and 6 eV DOSs for configurations 4 and 1 are plotted. Interestingly, the larger  $U-J=0$  spin-orbit interaction in configuration 4 is manifested by the spin-orbit splitting of its  $4f$  peaks which does not occur for configuration 1.

In summary, stimulated by the experimental determination<sup>6</sup> of the spin configuration of  $\text{GdB}_4$  we made extensive calculations and determined that for a wide range of Hubbard  $U$  values, the calculated ground state had collinear spins, resulting in a slight orthorhombic distortion rather than being tetragonal, as apparently assumed in Ref. 6 and having the noncollinear configuration determined there, but in agreement with the interpretation of the x-ray data in Ref. 5. Be-

TABLE VI. Magnetic groups of the space group  $P4/m\bar{b}m$ . The first column corresponds to the spin arrangement in Fig. 1. The following are the international notation, the factor group, and its members. Boldface italic operations contain a nonprimitive translation.

1	$4/m\bar{b}m$	$D_4$	$E, C_2, 2C_4, 2C_2', 2C_2''$
2	$4/m\bar{b}m$	$D_{2d}$	$E, C_2, 2S_4, 2\sigma_d, 2C_2'$
3	$4/m\bar{b}m$	$D_{2d}$	$E, C_2, 2S_4, 2\sigma_v, 2C_2''$
4	$4/m\bar{m}m$	$C_{4v}$	$E, C_2, 2C_4, 2\sigma_d, 2\sigma_v$
5	$4/m\bar{b}m$	$D_{2h}$	$E, C_2, 2C_2', i, \sigma_h, 2\sigma_v$

cause all density functionals are approximate and because the energy differences are so small, we cannot claim to have disproved the experimental result. In fact, if lattice constants and atomic positions obtained at 2.2 K were used in the interpretation of the experimental data, that interpretation is much more likely, than the theoretical result, to be correct. Nevertheless, taking into consideration the essentially perfect agreement between the calculated and measured lattice constants and especially the agreement of the magnitudes of the magnetizations with experiment, we believe that the 2.8 meV difference in total energy between these two states is significant enough to warrant further experimental and theoretical investigation.

#### ACKNOWLEDGMENTS

This work was supported by the Welch Foundation (Houston, TX) under Grant No. F-0934 and the Texas Advanced Computing Center (TACC), University of Texas at Austin. Useful conversation with B. R. Sahu is gratefully acknowledged.

#### APPENDIX

The space group of  $\text{GdB}_4$  above the transition temperature is  $P4/m\bar{b}m$  (No. 127). It contains the following operations:  $E, C_2, 2C_4, 2C_2', 2C_2'', i, \sigma_h, 2S_4, 2\sigma_v, 2\sigma_d$ , where those operations listed in boldface italic contain nonprimitive translations of  $(a/2, a/2, 0)$ , as shown in Table VI. A magnetic (or color) group consists of a factor group of order 2 plus the remaining group operations coupled with time reversal. The color groups for the first five configurations shown in Fig. 1 are listed in Table VI with their factor group operations. Note that the  $D_{2d}$  factor group occurs in two different color groups. In one case it contains  $\sigma_v$  and  $C'$  and in the other,  $C_2''$  and  $\sigma_d$ . For completeness, we note that there exists a  $4/m\bar{b}m$  color group formed from the  $C_{4h}$  factor group, but magnetic atoms in the  $4(g)$  sites cannot transform according to it.

- \*Present address: National Renewable Energy Laboratory, Golden, CO 80401.
- <sup>1</sup>M. A. Ruderman and C. Kittel, Phys. Rev. **96**, 99 (1954).
  - <sup>2</sup>J. Etourneau, J. Less-Common Met. **110**, 267 (1985).
  - <sup>3</sup>D. B. Ghosh, M. De, and S. K. De, Phys. Rev. B **72**, 045140 (2005).
  - <sup>4</sup>Z. Fisk, M. B. Maple, D. C. Johnston, and L. D. Woolf, Solid State Commun. **39**, 1189 (1981).
  - <sup>5</sup>S. W. Lovesey, J. Fernández Rodríguez, J. A. Blanco, and P. J. Brown, Phys. Rev. B **70**, 172414 (2004).
  - <sup>6</sup>J. A. Blanco, P. J. Brown, A. Stunault, K. Katsumata, F. Iga, and S. Michimura, Phys. Rev. B **73**, 212411 (2006).
  - <sup>7</sup>M. T. Garland, J. P. Wiff, J. Bauer, R. Guérin, and J.-Y. Saillard, Solid State Sci. **5**, 705 (2003).
  - <sup>8</sup>S. Ji, C. Song, J. Koo, K.-B. Lee, Y. J. Park, J. Y. Kim, J.-H. Park, H. J. Shin, J. S. Rhyee, B. H. Oh, and B. K. Cho, Phys. Rev. Lett. **91**, 257205 (2003).
  - <sup>9</sup>J. Fernández-Rodríguez, J. A. Blanco, P. J. Brown, K. Katsumata, A. Kikkawa, F. Iga, and S. Michimura, Phys. Rev. B **72**, 052407 (2005).
  - <sup>10</sup>D. M. Bylander and Leonard Kleinman, Phys. Rev. B **49**, 1608 (1994).
  - <sup>11</sup>D. M. Bylander and Leonard Kleinman, Phys. Rev. B, **50**, 1363 (1994).
  - <sup>12</sup>D. M. Bylander and Leonard Kleinman, Phys. Rev. B **50**, 4996 (1994).
  - <sup>13</sup>David Vanderbilt, Phys. Rev. B **41**, 7892 (1990).
  - <sup>14</sup>M. Petersen, Jurgen Hafner, and M. Marsman, J. Phys.: Condens. Matter **18**, 7021 (2006).
  - <sup>15</sup>G. Kresse and D. Joubert, Phys. Rev. B **59**, 1758 (1999).
  - <sup>16</sup>G. Kresse and J. Hafner, Phys. Rev. B **47**, 558 (1993); **49**, 14251 (1994).
  - <sup>17</sup>G. Kresse and J. Furthmüller, Comput. Mater. Sci. **6**, 15 (1996).
  - <sup>18</sup>G. Kresse and J. Furthmüller, Phys. Rev. B **54**, 11169 (1996).
  - <sup>19</sup>P. E. Blöchl, Phys. Rev. B **50**, 17953 (1994).
  - <sup>20</sup>S. L. Dudarev, G. A. Botton, S. Y. Savrasov, C. J. Humphreys, and A. P. Sutton, Phys. Rev. B **57**, 1505 (1998).
  - <sup>21</sup>M. Wierzbowska, A. Delin, and Erio Tosatti, Phys. Rev. B **72**, 035439 (2005).
  - <sup>22</sup>D. Hobbs, G. Kresse, and J. Hafner, Phys. Rev. B **62**, 11556 (2000).
  - <sup>23</sup>J. P. Perdew, J. A. Chevary, S. H. Vosko, K. A. Jackdon, M. R. Pederson, D. J. Singh, and C. Fiolhais, Phys. Rev. B **46**, 6671 (1992).
  - <sup>24</sup>M. Methfessel and A. T. Paxton, Phys. Rev. B **40**, 3616 (1989).
  - <sup>25</sup>Consider the upper left atom (ULA) in the unit cells in Fig. 1. The two-third neighbors have spin parallel to the ULA and lie in the planes above and below it. The two experimental second (although calculated first) neighbors seen in the unit cell are polarized at angles of  $\pi/2$  and  $3\pi/2$  with respect to the polarization of the ULA, as are the other two experimental second neighbors obtained from them by  $(0, a, 0)$  and  $(-a, 0, 0)$  translations, and therefore  $J_2$  plays no role in the polarization of the ULA. The experimental first neighbor (calculated second neighbor) with polarization antiparallel to the ULA is obtained from a  $(0, a, 0)$  translation of the atom in the unit cell farthest from the ULA. We will refer to the atoms in these positions as neighbors 3, 1, and 2, respectively.
  - <sup>26</sup>These are VASP cohesive energies which subtract off nonspin polarized atomic energies.